DispatchDate: 24.10.2020 · ProofNo: 809, p.1

nature plants

LETTERS

https://doi.org/10.1038/s41477-020-00809-6

HOS1 activates DNA repair systems to enhance plant thermotolerance

Shin-Hee Han[1], Young-Joon Park[1] and Chung-Mo Park[1,2] ✉

Plants possess an astonishing capability of effectively adapting to a wide range of temperatures, ranging from freezing to near-boiling temperatures[1,2]. Yet, heat is a critical obstacle to plant survival. The deleterious effects of heat shock on cell function include misfolding of cellular proteins, disruption of cytoskeletons and membranes, and disordering of RNA metabolism and genome integrity[3–5]. Plants stimulate diverse heat shock response pathways in response to abrupt temperature increases. While it is known that stressful high temperatures disturb genome integrity by causing nucleotide modifications and strand breakages or impeding DNA repair[6], it is largely unexplored how plants cope with heat-induced DNA damages. Here, we demonstrated that high expression of osmotically reponsive genes 1 (HOS1) induces thermotolerance by activating DNA repair components. Thermotolerance and DNA repair capacity were significantly reduced in HOS1-deficient mutants, in which thermal induction of genes encoding DNA repair systems, such as the DNA helicase RECQ2, was markedly decreased. Notably, HOS1 proteins were thermostabilized in a heat shock factor A1/heat shock protein 90 (HSP90)-dependent manner. Our data indicate that the thermoresponsive HSP90-HOS1-RECQ2 module contributes to sustaining genome integrity during the acquisition of thermotolerance, providing a distinct molecular link between DNA repair and thermotolerance.

During the course of analysing the pleiotropic phenotypes of HOS1-deficient mutants[7–9], we found that the *hos1-3* and *hos1-5* mutants showed a significantly reduced thermotolerance compared to that observed in wild-type Col-0 seedlings (Fig. 1a–c). Electrolyte leakage assays showed that cellular integrity was disturbed more severely in the mutants following heat shock (Fig. 1d). In contrast, transgenic overexpression of *HOS1* gene enhanced thermotolerance (Extended Data Fig. 1). On the other hand, the *hos1-3* mutant still showed acquired thermotolerance, comparable to that observed in Col-0 seedlings (Supplementary Fig. 1). These obse rvations indicate that HOS1 is functionally associated with basal thermotolerance but not linked with acquired thermotolerance.

Thermomorphogenic traits, such as elongated hypocotyls and leaf hyponasty, enhance leaf cooling under warm environments[10,11]. HOS1 attenuates hypocotyl thermomorphogenesis by suppressing the activity of PHYTOCHROME INTERACTING FACTOR 4 (PIF4)[12]. Infrared thermal imaging of heat-treated seedlings revealed that leaf temperatures were not discernibly different in Col-0 and *hos1-3* seedlings (Supplementary Fig. 2a,b). In addition, the *hos1-3 pif4-101* double mutant still showed a reduced thermotolerance, like the *hos1-3* mutant (Supplementary Fig. 2c,d). Conversely, it has been reported that the thermomorphogenic hypocotyl growth of the *hos1-3* mutant was compromised in the double mutant[12]. The previous and our own observations indicate that the HOS1-mediated thermotolerance is independent of PIF4.

HOS1 possesses a RING-finger domain, which is essential for its ubiquitin ligase activity[7]. It is known that the enzyme activity of HOS1 is disrupted by H75Y and C89S substitutions[13]. Transgenic production of a modified protein (mHOS1) harbouring the residue substitutions in the *hos1-3* mutant efficiently rescued the disturbed thermotolerance (Fig. 1e and Supplementary Fig. 3), showing that the enzyme activity is not necessary for the HOS1 function during thermotolerance.

Plant responses to heat stress are often mediated by reactive oxygen species (ROS)[14]. We observed that ROS accumulated to similar levels in Col-0 and *hos1-3* seedlings at high temperatures (Supplementary Fig. 4a). Histochemical detection of hydrogen peroxide and superoxide radicals further supported that ROS accumulation is not functionally linked with the HOS1-mediated thermotolerance (Supplementary Fig. 4b,c).

To obtain molecular insights into how HOS1 regulates thermotolerance, we used RNA sequencing analysis. The transcription of numerous genes was altered at high temperatures, and the discrepancy of global gene expression profiles between Col-0 and *hos1-3* seedlings was more prominent at high temperatures (Fig. 2a), suggesting that HOS1 mediates the transcriptional control of thermal responses. Analysis of gene ontology (GO) enrichment revealed that many genes belonging to diverse cellular, metabolic and adaptive processes were differentially expressed in the mutant (Fig. 2b). In particular, genes related to DNA repair responses were thermally upregulated in Col-0 seedlings but their thermal regulation was largely compromised in the *hos1-3* seedlings (Fig. 2b–d). Accordingly, comparative analysis of DNA integrity by comet assay, which is widely used to visualize DNA damages[15], revealed that DNA damages were more prominent in the *hos1-3* seedlings, especially at high temperatures, than in Col-0 seedlings (Fig. 2e). Together, these observations indicate that HOS1 is involved in the maintenance of genomic integrity under heat stress.

We next examined the thermotolerance phenotypes of DNA damage response-related mutants. Among the mutants tested, the RECQ2-deficient *recq2* mutant showed the most prominent reduction of thermotolerance (Fig. 3a–c and Extended Data Fig. 2a). In addition, DNA damages were more severe in the mutant at high temperatures (Fig. 3d), suggesting that RECQ2 is involved in the HOS1-mediated maintenance of genomic integrity at high temperatures. The RECQ2 DNA helicase unwinds the displacement loop of homologous recombination intermediates in vitro and it has been predicted to act as a component of DNA repair pathways[16]. It physically interacts with the Werner syndrome-like exonuclease exonuclease (AtWRNexo)[17]. We observed that the AtWRNexo-deficient mutant did not show altered thermotolerance (Extended Data

[1]Department of Chemistry, Seoul National University, Seoul, Korea. [2]Plant Genomics and Breeding Institute, Seoul National University, Seoul, Korea. ✉e-mail: cmpark@snu.ac.kr

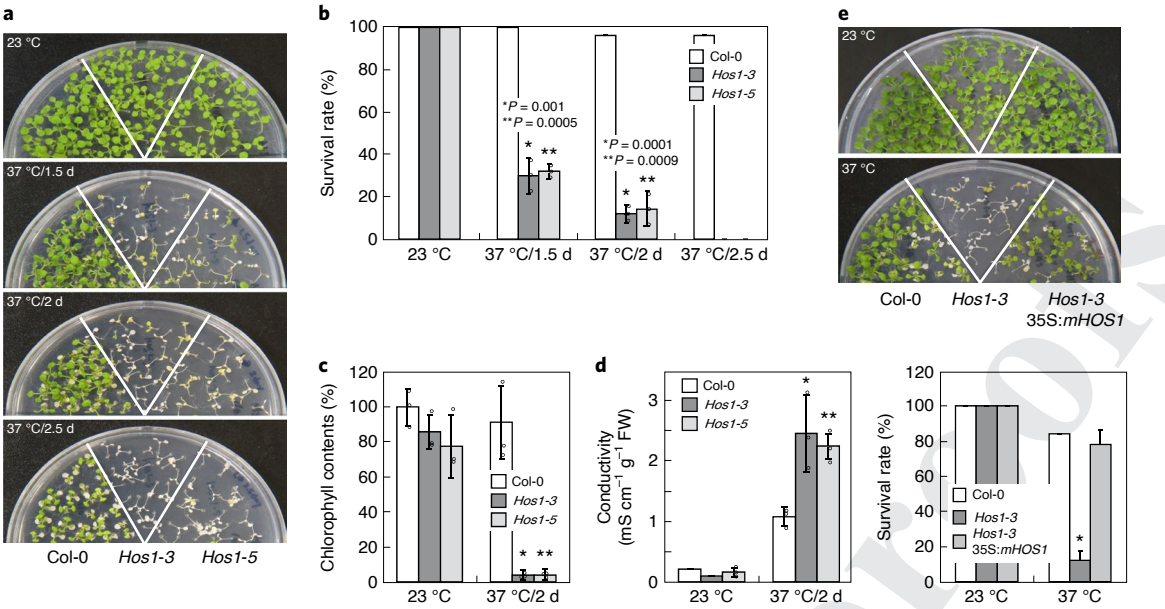

Fig. 1 | HOS1 is required for the acquisition of thermotolerance. Two independent HOS1-deficient lines, *hos1-3* and *hos1-5*, were assayed. **a**–**d**, Seven-day-old seedlings grown on MS-agar plates at 23 °C were exposed to 37 °C for the indicated durations. Three measurements, each consisting of 15–20 seedlings, were statistically analysed using one-sided Student's *t*-test (**c**, $*P = 0.01917$, $**P = 0.01722$; **d**, $*P = 0.034$, $**P = 0.013$, difference from Col-0). **b**–**d**, Error bars indicate s.e.m; circles indicate individual datapoints. **a**–**c**, Thermotolerance phenotypes of *hos1* mutants. Heat-treated seedlings were allowed to recover at 23 °C for 5 d under constant light conditions before taking photographs shown in **a**. Survival rates (**b**) and relative chlorophyll contents (**c**) were measured. **d**, Electrolyte leakage assays. Conductivity was measured using seedlings that were allowed to recover at 23 °C for 2 d following heat treatments. **e**, Complementation of *hos1-3* mutant. A gene sequence encoding the modified HOS1 protein (mHOS1) harbouring H75Y and C89S substitutions was overexpressed driven by the cauliflower mosaic virus (CaMV) 35S promoter in the *hos1-3* mutant. Three measurements, each consisting of 15–20 seedlings, were statistically analysed using one-sided Student's *t*-test ($*P = 0.0005$, difference from Col-0). Error bars indicate s.e.m.

Fig. 2b), unlike the *recq2* mutant, suggesting that AtWRNexo is not functionally associated with the HOS1-mediated thermotolerance.

Our data indicate that HOS1 is related to the thermal induction of *RECQ2* gene. To investigate how HOS1 mediates the *RECQ2* transcription, we first used chromatin immunoprecipitation (ChIP)–qPCR assays using a set of conserved sequence regions containing G-box and GATA-box in the *RECQ2* promoter (P1–P5 in Fig. 3e and Extended Data Fig. 3a). We found that HOS1 highly enriched *RECQ2* chromatin domains harbouring P3 and P5 sequences at high temperatures (Fig. 3f and Extended Data Fig. 3b).

While HOS1 lacks any distinct DNA-binding motifs and its direct binding to DNA is not proven[18,19], it acts as a chromatin modifier through physical interactions with HISTONE DEACETYLASE 6 (HDA6) and HDA15 in modulating the epigenetic control of *FLOWERING LOCUS C* transcription during thermosensory flowering[9]. We found that *Arabidopsis* mutants lacking HDA6 or HDA15 showed a thermotolerance phenotype indistinguishable from that of Col-0 seedlings (Supplementary Fig. 5a-c), indicating that the HOS1-HDA6/15 complex-mediated epigenetic control is not involved in the development of thermotolerance. Consistently, the patterns of histone modifications were unaltered in the *RECQ2* chromatin at high temperatures (Fig. 3g and Supplementary Fig. 5d).

HOS1 acts as a transcriptional coregulator through interactions with transcription factors, such as PIF4 (ref. [12]). Transcriptional activation activity assays in *Arabidopsis* protoplasts showed that expression of a full-size *HOS1* gene, but not the N-terminally and C-terminally truncated forms, led to the induction of the β-glucuronidase reporter gene (Fig. 3h). Together with the association of HOS1 with *RECQ2* chromatin, these observations indicate that HOS1 acts as a transcriptional coregulator of *RECQ2* gene and both the N terminal and C terminal domains are required for its transactivation activity.

To verify the functional relationship between HOS1 and RECQ2, we produced *hos1-3 recq2* double mutant by cross. We observed that the thermotolerance of the double mutant was comparable to that of the *hos1*-3 mutant (Fig. 3i and Extended Data Fig. 4), demonstrating that the *HOS1* and *RECQ2* genes constitute a single genetic pathway in regulating thermotolerance. In addition, overexpression of *RECQ2* gene in the *hos1-3* mutant restored the reduced thermotolerance (Fig. 3j), further supporting the HOS1-RECQ2 linkage. The incomplete complementation of the *hos1-3* thermotolerance phenotypes by *RECQ2* overexpression would be because HOS1 also regulates other targets in addition to *RECQ2*.

We next examined the functional significance of HOS1 and RECQ2 in triggering DNA repair response by using genotoxins, such as *cis*-diamminedichloroplatinum (II) and mitomycin C (MMC), which damage DNA molecules by triggering cross-linking of nucleotides[20]. Both the *hos1-3* and *recq2* seedlings were more sensitive to these genotoxins than Col-0 seedlings at high temperatures (Fig. 3k,l and Extended Data Fig. 5), signifying the regulatory roles of HOS1 and RECQ2 in triggering DNA repair response under heat stress. Consistent with a previous report that DNA damages induce cell death[21], trypan blue exclusion test, which selectively stains dead cells[22], showed that cell death was more widespread in the mutant leaves than in Col-0 leaves (Supplementary Fig. 6).

A key question was how HOS1 incorporates thermal signals into the transcriptional control of DNA repair genes. HSPs and their upstream transcriptional regulators, heat shock factors (HSFs), play critical roles in the development of thermotolerance[23]. We found that the levels of *HSP* and *HSF* transcripts were not discernibly altered in the *hos1-3* seedlings (Supplementary Fig. 7a). The protein abundance of HSP90 was also unaffected in the mutants at high temperatures (Supplementary Fig. 7b), indicating that HOS1 does

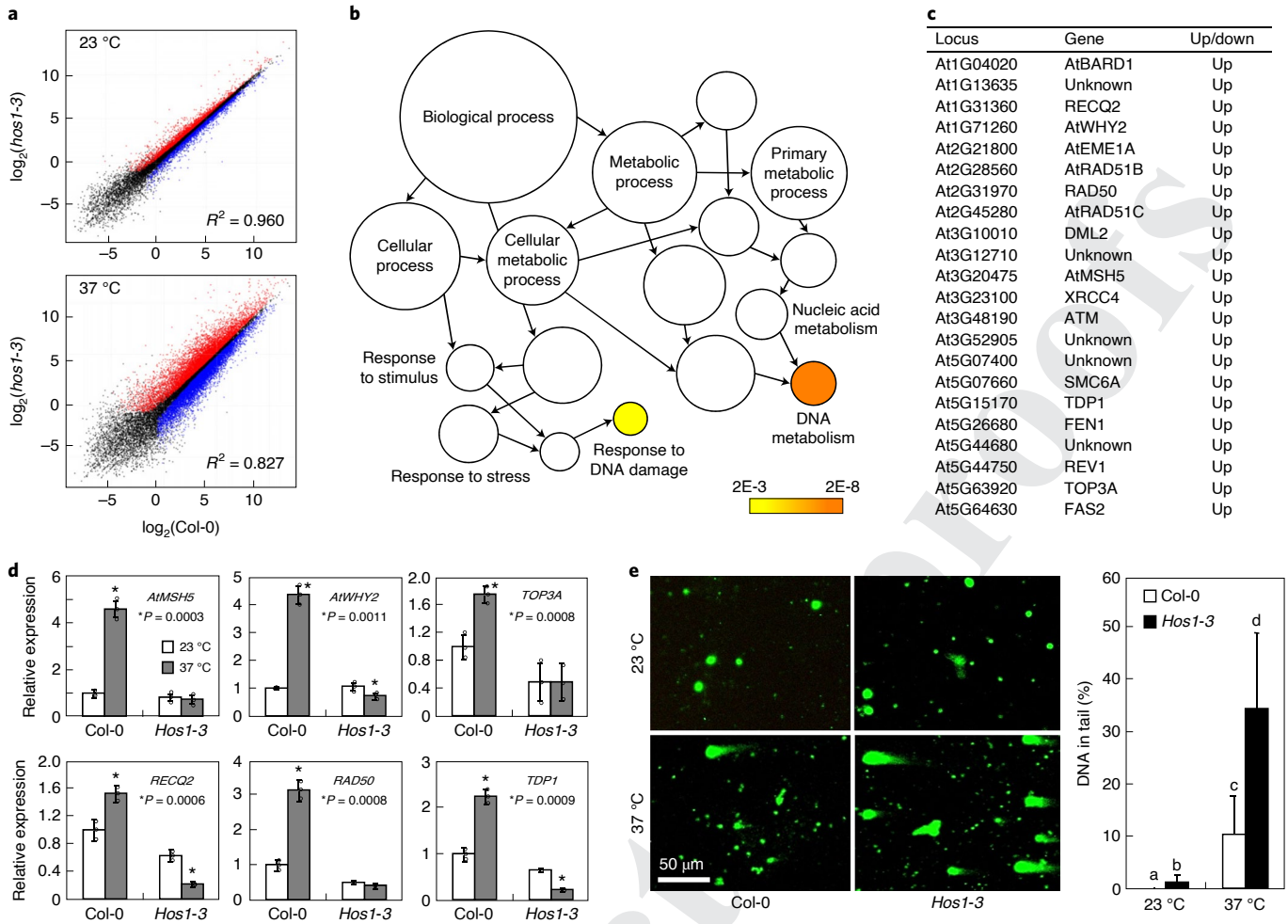

Fig. 2 | DNA damage response is reduced in *hos1-3* mutant at high temperatures. a, Scatter plots of related gene expression values obtained by RNA sequencing analysis. Seven-day-old seedlings grown on MS-agar plates at 23 °C were exposed to 37 °C for 1.5 d. Total RNA samples were extracted from whole seedlings. Biological triplicates, each consisting of ten seedlings, were statistically analysed. Expression values were plotted between Col-0 wild type and *hos1-3* mutant seedlings. Blue spots indicate genes downregulated in the *hos1-3* seedlings. Red spots indicate those upregulated in the mutant seedlings. Black spots indicate those unaltered in the mutant seedlings. **b**, GO analysis of HOS1-regulated genes at high temperatures. The network diagram visualizes the results of analysis using the Biological Networks Gene Ontology tool. **c**, Thermal induction of DNA damage response genes. The selected genes were thermoinduced by more than fourfold in Col-0 seedlings but the thermal induction largely disappeared in the *hos1-3* seedlings. Among 292 genes thermally induced by more than fourfold, 22 genes were predicted to be involved in DNA repair response. **d**, qRT–PCR analysis of selected DNA damage response genes. Biological triplicates, each consisting of 15 seedlings, were statistically analysed using one-sided Student's *t*-test (*$P < 0.01$, difference from 23 °C). The upper side of each boxplot indicates median. Error bars indicate s.e.m. The circles indicate individual datapoints. **e**, Comet assays on heat-treated seedlings. Seedling growth and heat treatments were performed, as described in **a**. DNA breaks were quantitated by measuring the tail ratio of total fluorescence intensity in comet-shaped DNA spots using the casplab program (http://casplab.com/). DNA spots in a range of 8–12 were statistically analysed. Error bars indicate standard deviation from the mean (s.d.). Different letters represent significant differences ($P < 0.01$) determined by one-way ANOVA with post hoc Tukey test.

not affect the expression of *HSP* and *HSF* genes and the accumulation of their encoded proteins under heat stress.

Notably, protein accumulation assays revealed that the levels of HOS1 were rapidly elevated by more than fivefold following heat exposure (Fig. 4a). Moreover, the HOS1 levels were elevated by approximately threefold in the presence of MG132 at normal temperatures (Fig. 4b). These observations point out that HOS1 abundance is maintained at a relatively low level through the 26S proteasome-mediated degradation at normal temperatures but the degradation pathways are suppressed at high temperatures. In the meantime, the transcription of *HOS1* gene was elevated by less than twofold at high temperatures (Supplementary Fig. 8). It is thus likely that the thermal activation of HOS1 function is exerted mainly at the protein level.

HSPs act as molecular chaperones that stabilize cellular proteins, including DNA-modifying enzymes[24], during plant thermal responses[25]. It was notable that the thermal accumulation of HOS1 was largely attenuated in the presence of HSP90 inhibitors, geldanamycin (GDA) and radicicol (Fig. 4c and Extended Data Fig. 6a). In addition, DNA breaks were more prominent when seedlings were treated with HSP90 inhibitors (Fig. 4d and Extended Data Fig. 6b). Furthermore, the HOS1 thermostabilization was largely eliminated in the *HSP90*-RNAi plants (Fig. 4e), which showed a significant reduction in thermotolerance and thermal induction of *RECQ2* transcription (Extended Data Fig. 7). These observations indicate that HSP90 mediates the thermostabilization of HOS1. Consistent with the role of HSP90 in the HOS1-mediated thermotolerance, radicicol treatments reduced thermotolerance by approximately

80% in Col-0 seedlings (Extended Data Fig. 8). Thermotolerance was also reduced, but to a lesser degree, in the *hos1-3* mutant when treated with radicicol, suggesting that HOS1 is not the sole target of HSP90 in inducing thermotolerance.

It has been reported that the thermal accumulation of HSP90 proteins is markedly reduced in the *hsfa1a hsfa1b hsfa1d hsfa1e* quadruple knockout (*hsfa1* QK) mutant, which lacks HSF master regulators[26]. We found that the thermal accumulation of HOS1 was drastically reduced in the *hsfa1* QK mutant (Fig. 4f). In addition, the *hsfa1* QK mutant seedlings showed a marked reduction in thermotolerance and thermal induction of *RECQ2* transcription (Extended Data Fig. 9), similar to what observed in the *HSP90*-RNA interference plants (Extended Data Fig. 7). Accordingly, DNA breaks were significantly elevated in the *hsfa1* QK mutant (Fig. 4g), showing that the HSFA1-HSP90 module mediates the stabilization of HOS1 in the acquisition of thermotolerance. However, we did not detect any direct interactions between HSP90 and HOS1 in yeast cells (Supplementary Fig. 9a) and bimolecular fluorescence complementation assays (Supplementary Fig. 9b), raising a possibility that additional chaperone(s) or cochaperone(s) would be required for the HOS1 thermostabilization.

A critical issue regarding the thermoregulatory role of HOS1 is whether it regulates additional DNA repair genes other than *RECQ2* in maintaining genomic integrity. Ultraviolet hypersensitive 6 (UVH6) is a DNA repair helicase and UVH6-deficient mutants are hypersensitive to ultraviolet light (UV) and heat stress[27]. While the *UVH6* gene was not identified as a differentially expressed gene in our RNA sequencing analysis, possibly because of technical limits in the identification process, we examined its potential involvement in the HOS1-mediated thermotolerance. The *UVH6* transcription was elevated by more than fourfold at high temperatures, but its thermal induction largely disappeared in the *hos1-3* mutant (Extended Data Fig. 10a). In addition, thermotolerance was significantly reduced in the UVH6-deficient mutant (Extended Data Fig. 10b). It is therefore envisaged that HOS1 mediates the thermal regulation of multiple DNA repair genes during thermotolerance.

DNA damages include various chemical alterations that disrupt genomic integrity in plants[28]. Here, we demonstrate that HOS1 functions as a transcriptional coregulator of DNA repair genes during the establishment of basal thermotolerance, directly linking DNA repair to thermotolerance (Fig. 4h). However, HOS1 is not related with acquired thermotolerance, which often depends on heat stress memory mostly through chromatin modifications[29]. This view is supported by the lack of discernible histone modifications in *RECQ2* chromatin at high temperatures (Fig. 3g and Supplementary Fig. 5d). Our data also explain why RECQ2 have not been functionally defined by mutant analysis at normal temperatures[20].

Recent studies show that HOS1 also acts as a chromatin modifier and a component of nuclear pore complexes[9,30]. It is possible that HOS1 mediates the epigenetic control of DNA repair genes and/or the nucleocytoplasmic transport of their messenger RNAs and proteins. It is notable that the widely conserved HSP90 thermostabilizes HOS1 during thermotolerance. It is known that the functions of HSPs are not confined to molecular chaperone activities; they also act as constituents of metabolic enzymes and regulatory proteins during various developmental and adaptive processes[31]. Our findings would further broaden our understanding of HSP-mediated stress adaptation in plants.

Methods

Plant materials and growth conditions. All *Arabidopsis thaliana* lines used were in Columbia (Col-0) background, unless specified otherwise. Sterilized seeds were cold-imbibed (4 °C) in darkness for 3 d and allowed to germinate on ½ × Murashige and Skoog-agar (hereafter referred to as MS-agar) plates under long days (LDs, 16-h light and 8-h dark). White light illumination was provided at light intensity of 120 µmol photons $m^{-2}s^{-1}$ using fluorescent FLR40D/A tubes (Osram). Plants were grown in a controlled culture room set at 23 °C with relative humidity of 60%.

The transfer DNA insertional knockout mutants, *hos1-3, hos1-5, pif4-101, hos1-3 pif4-101, hda6* and *hda15-1*, have been described previously[9,12]. The *hsfa1a hsfa1b hsfa1d hsfa1e* quadruple knockout (*hsfa1* QK) mutants in Col-0 and Ws-2 background have been described previously[23]. The 35S:*MYC-HOS1* transgenic plants have been described previously[9]. The RECQ2-deficient *recq2* mutant (SALK-087178.32.55) was isolated from a pool of T-DNA insertional lines deposited in the *Arabidopsis* Biological Resource Center. The *atwhy2* (SAIL-694-A11), *atr* (SALK-032841.54.00), *tdp1* (WiscDsLox361D04), *top3a-2* (GABI-476A12), *uvh6* (SALK-006580) and *wrnexo* (SALK-003278) mutants were also isolated from the mutant pool deposited in the ABRC. The *hos1-3 recq2* double mutant was generated by crossing *hos1-3* and *recq2* mutants. A gene encoding a modified HOS1 protein (mHOS1) harbouring H75Y and C89S substitutions was

Fig. 3 | HOS1 mediates the thermal induction of *RECQ2* gene during thermotolerance response. a–c, Thermotolerance phenotypes of *recq2* mutant. Seven-day-old seedlings grown on MS-agar plates at 23 °C were exposed to 37 °C for 1.5 d and allowed to recover at 23 °C for 5 d under constant light conditions (**a**). Survival rates (**b**) and chlorophyll contents (**c**) were measured. Biological triplicates, each consisting of 50 (**b**) or 10 (**c**) seedlings, were statistically analysed (one-sided *t*-test, $*P = 0.003$ (**b**) or 0.008 (**c**), difference from Col-0). The upper side of each boxplot indicates median. Error bars indicate s.e.m. The circles indicate individual datapoints. **d**, Comet assays on *recq2* mutant. The assays were performed and statistically analysed, as described in Fig. 2e. DNA spots of 8–12 were statistically analysed. Different letters represent significant differences ($P < 0.01$) determined by one-way ANOVA with post hoc Tukey test. Error bars indicate s.d. **e**, Sequence elements in *RECQ2* promoter. The P1–P5 sequence regions were chosen for ChIP–qPCR assays. **f**, Binding of HOS1 to *RECQ2* chromatin. ChIP–qPCR assays were performed using the 35S:*MYC-HOS1* transgenic plants. Five measurements were statistically analysed (one-sided *t*-test, difference from MYC only). Error bars indicate s.d. The *YUC8* promoter sequence was included as positive control in the assays. The circles indicate individual datapoints. **g**, Histone modifications at *RECQ2* chromatin. Seven-day-old seedlings were used. An anti-H3Ac was used for immunoprecipitation. Histone modifications in the P5 sequence were analysed by ChIP–qPCR. Three measurements were statistically analysed (one-sided *t*-test, $*P < 0.05$, difference from 23 °C). The upper side of each boxplot indicates median. Error bars indicate s.d. The circles indicate individual datapoints. **h**, Transcriptional activation activity assays in *Arabidopsis* protoplasts. A set of reporter and effector constructs was generated (upper diagram). The vectors were cotransformed into *Arabidopsis* protoplasts. The 35S promoter-luciferase construct was included as internal control in the assays. Relative GUS activities were determined fluorimetrically (lower graph). ARF5M was positive control. A full-size (HOS1-F, residues 1–927), a C-terminally truncated (HOS1-N, residues 1–457) and an N-terminally truncated (HOS1-C, residues 457–927) HOS1 forms were assayed. Five measurements were statistically analysed (one-sided *t*-test, $*P = 0.00821$, $**P = 0.00367$, difference from control). The upper side of each boxplot indicates median. Error bars indicate s.d. The circles indicate individual datapoints. **i**, Thermotolerance phenotypes of *hos1-3 recq2* mutant. Seedlings were exposed to 37 °C for 1.25 d. **j**, Thermotolerance phenotypes of *hos1-3 RECQ2*-ox plants. A RECQ2-coding sequence was overexpressed driven by the CaMV 35S promoter in the *hos1-3* mutant. Seedlings were exposed to 37 °C for 2 d and allowed to recover at 23 °C for 3 d under constant light conditions. **i**,**j**, Three measurements, each consisting of 20 seedlings, were statistically analysed. Error bars indicate s.e.m. Different letters represent significant differences ($P < 0.01$) determined by one-way ANOVA with post hoc Tukey test. The circles indicate individual datapoints. **k**,**l**, Thermotolerance phenotypes of *hos1-3* (**k**) and *recq2* (**l**) mutants in the presence of cisplatin. Seven-day-old seedlings grown on MS-agar plates at 23 °C were transferred to liquid MS cultures containing 10 mM cisplatin (cis) and exposed to 37 °C for 20 h. Heat-treated seedlings were allowed to recover at 23 °C for 10 d under constant light conditions. Three measurements, each consisting of 20 seedlings, were statistically analysed. Error bars indicate s.e.m. Different letters represent significant differences ($P < 0.05$) determined by two-way ANOVA with post hoc Fisher's multiple comparison test. The circles indicate individual datapoints.

expressed driven by the cauliflower mosaic virus (CaMV) 35S promoter using the myc-pBA vector in the *hos1-3* mutant[32]. A RECQ2-coding complementary DNA was overexpressed driven by the CaMV 35S promoter in the *hos1-3* mutant using the pEarleyGate 203 vector[33].

Thermotolerance assay. Seven-day-old *Arabidopsis* seedlings grown on MS-agar plates at 23 °C under LDs were exposed to 37 °C for appropriate durations. The heat-treated seedlings were allowed to recover at 23 °C for 5 d under constant light conditions. For pharmacological treatments, GDA, an antibiotic that inhibits HSP90 function[34], was included at a final concentration of 10 μM in MS liquid, in which seedlings were floated during heat treatments. Radicicol, a macrolactone antibiotic that inhibits HSP90 function[35], was used at a final concentration of 10 μM. Cisplatin, a cross-linking agent, was used at a final concentration of 10 μM. MMC was used at a final concentration of 10 μg ml^{-1} (ref. [20]). MG132, a 26S proteasome inhibitor[36], was used at a final concentration of 10 μM. The pharmacological reagents were purchased from Sigma-Aldrich.

For analysis of electrolyte leakage, aerial parts of heat-treated seedlings were floated on 0.4 M sorbitol solution in darkness for 12 h, after which sample conductivity of the solution was measured. Then, the seedling sample solutions were boiled in the same solution for 5 min and total conductivity of the solution was measured. Electrolyte leakage is represented by relative conductivity, which is calculated by dividing sample conductivity by total conductivity. Conductivity was measured using the Orion 5-star conductivity meter (Thermo Fisher Scientific).

For measurements of chlorophyll contents, heat-treated seedlings were allowed to recover at 23 °C for 5 d under constant light conditions. Chlorophylls were extracted from the seedlings by soaking in 100% methanol at 4 °C for 2 h in complete darkness. Chlorophyll contents were analysed using the Mithras LB940 multimode microplate reader (Berthold Technologies). The absorbance data were collected using the MikroWin 2010 software (Berthold Technologies). The contents of chlorophyll *a* and chlorophyll *b* were calculated from the absorbance values at 650 and 660 nm (ref. [37]). Total chlorophyll contents were calculated by summing up those of chlorophyll *a* and chlorophyll *b*. Relative chlorophyll contents were calculated by dividing total chlorophyll contents of heat-treated seedlings by those of seedlings treated under mock conditions.

To examine the effects of heat acclimation on the HOS1-mediated induction of thermotolerance, 7-day-old seedlings were exposed to 37 °C for 2 h and incubated at 23 °C for 2 h before exposure to 45 °C for 7 h. The heat-treated seedlings were allowed to recover at 23 °C for 5 d under constant light conditions.

Gene expression analysis. Total RNA samples were extracted from 7-day-old seedlings grown on MS-agar plates and pretreated extensively with RNase-free DNase to get rid of genomic DNA contamination before use. RNA concentration was measured using the NanoDrop 2000 spectrophotometer (Thermo Fisher Scientific). Analysis of transcript levels was performed by quantitative PCR with reverse transcription (qRT–PCR) along with the rules proposed to assure reproducible and accurate measurements[38]. The qRT–PCR reactions were conducted in 384-well blocks with the Applied Biosystems QuantStudio 6 Flex Real-Time PCR System (Life Technologies) using the SYBR Green I master mix in a volume of 10 μl. A two-step thermal cycling profile used was 15 s at 95 °C for denaturation and 50 s at 60–65 °C, depending on the calculated

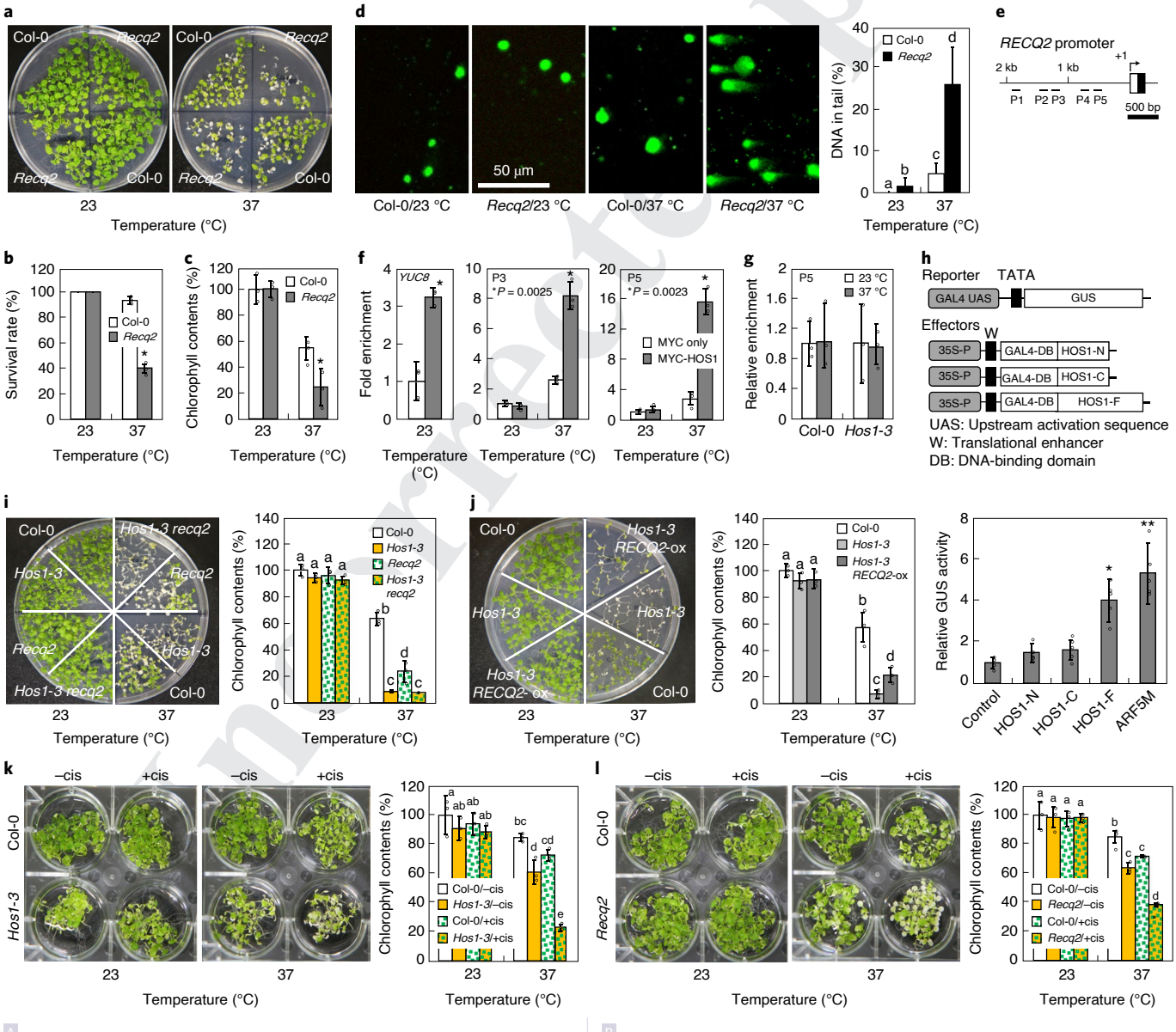

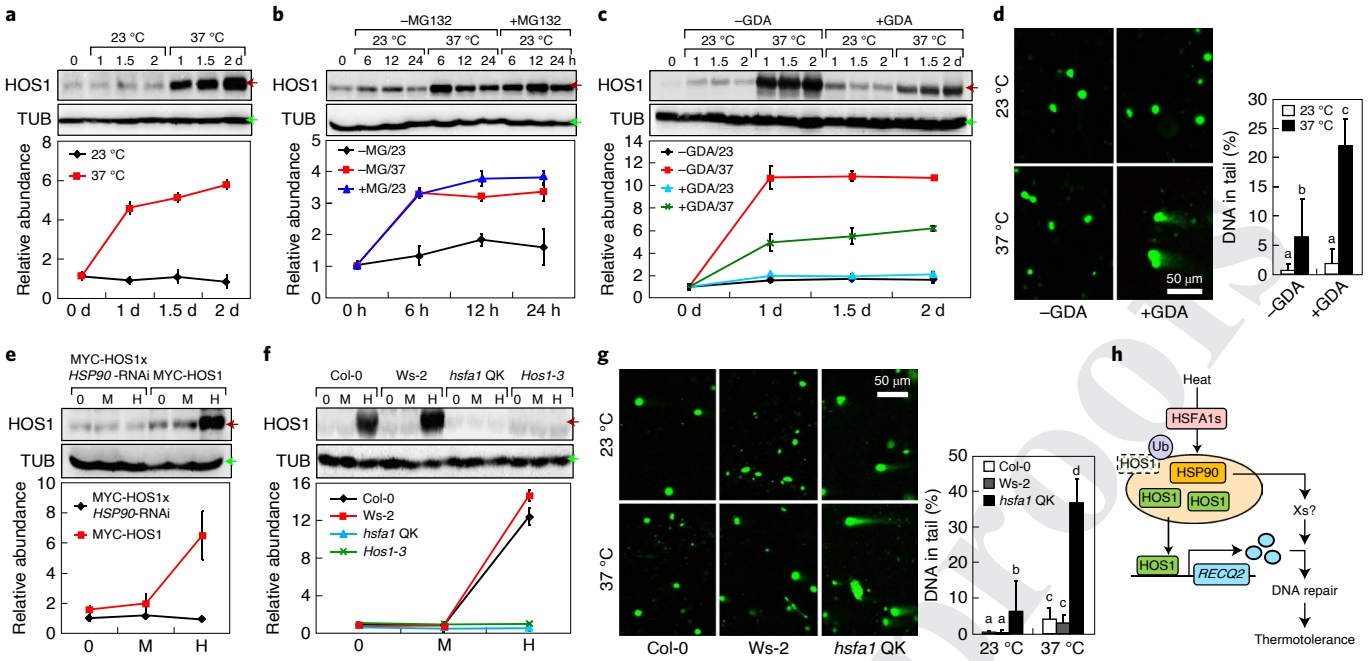

Fig. 4 | The HSFA1-HSP90-HOS1 module activates DNA repair response at high temperatures. a–c, Seven-day-old 35S:*MYC-HOS1* transgenic seedlings grown at 23 °C were exposed to 37 °C for varying durations in the presence of chemicals. Whole seedlings were used for the extraction of total proteins. Immunoblots were statistically analysed ($n = 3$ biologically independent samples). The dotplots indicate median. Error bars indicate s.d. Brown arrows mark 112 kDa and green arrows mark 50 kDa. **a**, Thermal stabilization of HOS1. The MYC-HOS1 proteins were immunologically detected using anti-MYC. TUB proteins were similarly analysed using anti-TUB for protein quality control. **b**, Effects of MG132 on HOS1 protein stability. Seedlings were incubated in liquid MS cultures containing 10 mM MG132. **c**, Effects of HSP90 inhibitor on thermal accumulation of HOS1. GDA was included at the final concentration of 10 mM. **d**, Comet assays in the presence of GDA. GDA was included at the final concentration of 10 mM in the assays. The tail ratio of total fluorescence intensity in comet-shaped DNA spots was quantitated using the casplab program. DNA spots of 8–12 were statistically analysed. Error bars indicate s.d. Different letters represent significant differences ($P < 0.01$) determined by one-way ANOVA with post hoc Tukey test. **e**, Thermal protein abundance of HOS1 in *HSP90*-RNAi plants. The *HSP90*-RNAi plant was crossed with the 35S:*MYC-HOS1* transgenic plant. Seedlings were incubated at either 23 °C (M) or 37 °C (H) for 1.5 d. An anti-MYC was used for the immunodetection of MYC-HOS1. Immunoblots were statistically analysed ($n = 3$ biologically independent samples). The dotplots indicate median. Error bars indicate s.d. Brown arrows mark 112 kDa and green arrows mark 50 kDa. **f**, Thermal protein abundance of HOS1 in the *hsfa1*QK mutant. The *hsfa1*QK seedlings were heat-treated for 6 h and anti-HOS1 was used for the immunodetection of HOS1. Immunoblots were statistically analysed ($n = 3$ biologically independent samples). The dotplots indicate median. Error bars indicate s.d. Brown arrows mark 105 kDa and green arrows mark 50 kDa. **g**, Comet assays on heat-treated *hsfa1*QK mutant. Seedling growth, heat treatments and comet assays were performed, as described in **d**. DNA spots of 8–12 were statistically analysed. Error bars indicate s.d. Different letters represent significant differences ($P < 0.01$) determined by one-way ANOVA with post hoc Tukey test. Biological triplicates, each consisting of ten DNA spots, were statistically analysed. Different letters represent significant differences ($P < 0.01$) determined by one-way ANOVA with post hoc Tukey test. **h**, Acquisition of thermotolerance via the HOS1-mediated activation of DNA repair response. HOS1 is stabilized via the HSP90 chaperone cycle at high temperatures, and the thermostabilized HOS1 activates the RECQ2 DNA helicase, thus leading to the establishment of thermotolerance. It seems that additional regulators (Xs) other than HOS1 are also involved in the RECQ2-mediated DNA repair response.

melting temperatures of PCR primer pairs used, for concomitant annealing and polymerization. PCR primers were designed using the Primer Express Software installed in the system and listed in Supplementary Table 1. An additional round of 10 min at 65 °C was provided at the end of individual thermal cycles for the completion of PCR reactions. An *eIF4A* gene (At3g13920) was included in the qRT–PCR reactions as internal control to standardize the differences in the amounts of cDNA samples used. Gene expression data collection and analysis were conducted using the QuantStudio Real-Time PCR v.1.1 software (Life Technologies).

All qRT–PCR reactions were performed using three independent RNA samples prepared from different plant samples grown under identical conditions. The comparative $\Delta\Delta C_T$ method was used to evaluate relative quantities of individual amplified products in the samples. The threshold cycle C_T was automatically determined for each reaction by the system set with default parameters. The specificity of the qRT–PCR reactions was determined by melt curve analysis of the amplified products using the standard method installed in the system.

Protein stability. Seven-day-old seedlings grown on MS-agar plates at 23 °C under LDs were exposed to 37 °C for varying durations. Whole seedlings were harvested for the extraction of total proteins. The MYC-HOS1 proteins were immunologically detected using anti-MYC (Millipore). The HOS1 proteins and HSP90 proteins were immunodetected using anti-HOS1 (AbClon) and anti-HSP90 (Millipore), respectively. TUBULIN (TUB) proteins were similarly immunodetected using anti-TUB for protein quality control. The horseradish peroxidase (HRP)-conjugated secondary antibodies, goat anti-mouse IgG-HRP and goat anti-rabbit IgG-HRP (Millipore), were used for chemiluminescent western blot detection. Gel images were collected using the Fusion Molecular Imaging v.15.18 software (Vilber Lourmat). Three independent biological samples were analysed per each assay.

RNA sequencing. Seven-day-old seedlings grown on MS-agar plates at 23 °C under LDs were exposed to 37 °C for 1.5 d. Total RNA samples were extracted from whole seedlings. The RNA samples were then subjected to RNA sequencing in Chunlab. Biological triplicates were statistically analysed. Genes with $P < 0.15$ and thermal induction by more than fourfold in Col-0 seedlings but no discernible thermal induction in *hos1-3* seedlings were regarded as differentially expressed genes. GO analysis was performed using the Biological Networks Gene Ontology tool (BiNGO) with Benjamini–Hochberg corrected $P < 0.01$. The network diagram shows significantly over-represented GO terms. The raw RNA-seq data were deposited in the NCBI SRA database with accession number PRJNA658831.

Comet assay. Comet assays were conducted, essentially as described previously[15]. Briefly, ~150 mg of plant materials were used for individual assays, which were performed in darkness. Microscopic slide glasses were coated with a layer of 1%

normal melting point agarose and dried at room temperatures. Seedlings were sliced with a razor blade in 400 µl PBS buffer (160 mM NaCl, 4 mM NaH_2PO_4, 8 mM Na_2HPO_4, pH 7.2) containing 50 mM EDTA. Two drops of nuclei suspension (approximately 40 µl each) were put separately on each slide, mixed with the same volume of 1% low melting point agarose at 42 °C and covered with cover glasses. Nuclei were then extracted using high salt buffer (2.5 M NaCl, 100 mM EDTA, 10 mM Tris-HCl, pH 7.3) for 20 min at room temperatures. Following equilibration for 5 min in 1 × TBE buffer (90 mM Tris-borate, 2 mM EDTA, pH 8.5) on ice, electrophoresis was performed at room temperatures using 1 × TBE running buffer at 30 V (1 V cm^{-1}, 15 mA) for 6 min. The gels were visualized by staining with SYBR Green I and photographed using the Carl Zeiss LSM510 confocal microscope. Comet images were processed using the Zen 2 software (blue edition, Carl Zeiss). Three independent biological samples, in which at least ten nuclei were photographed for each sample, were examined, and the data were analysed using the Casp-1.2.3b2 software (http://casplab.com/).

Chromatin immunoprecipitation. The ChIP assays were conducted, essentially as described previously[39]. Briefly, 10-day-old seedlings grown on MS-agar plates under LDs were vacuum-infiltrated with 1% (v/v) formaldehyde for cross-linking. The plant materials were thoroughly ground in liquid nitrogen after quenching the cross-linking process and resuspended in 30 ml of nuclear extraction buffer (1.7 M sucrose, 10 mM Tris-Cl, pH 7.5, 2 mM $MgCl_2$, 0.15% Triton-X-100, 5 mM β-mercaptoethanol, 0.1 mM PMSF) containing a mixture of protease inhibitors (Sigma-Aldrich). The resuspended sample was filtered through miracloth filters (Millipore) and centrifuged at 4,300*g* for 20 min at 4 °C. Nuclear fractions were isolated by the sucrose cushion method, lysed in lysis buffer (50 mM Tris-Cl, pH 8.0, 0.5 M EDTA, 1% SDS) containing a mixture of protease inhibitors, and sonicated to obtain chromatin fragments of 400–700 base pairs.

A total of 5 µg of anti-MYC (Millipore) was added to the chromatin preparation and incubated at 4 °C for 16 h. The protein G-agarose beads (Millipore) were then added to the solution for 1 h. The mixture was then centrifuged at 4,000*g* for 2 min at 4 °C. Following reverse cross-linking of the precipitates, residual proteins were removed using proteinase K. DNA fragments were purified using a silica membrane spin column (Promega). Quantitative PCR was performed to determine the amounts of DNA enriched in chromatin preparations and the values were normalized to the amount of input in each sample. For ChIP assays using anti-H3Ac (Millipore), the values were normalized to the amount of *eIF4A* DNA fragments in each sample.

Analysis of endogenous ROS contents. The 2',7'-dichlorodihydrofluorescein diacetate (H_2DCFDA, Sigma-Aldrich) fluorescent dye was used at a final concentration of 10 µM for the detection of hydrogen peroxide. For H_2DCFDA staining, cotyledons of 7-day-old seedlings were incubated in the H_2DCFDA staining solution for 20 min at room temperatures. The plant samples were then destained by washing thoroughly with deionized water and visualized by optical microscopy (Olympus). Microscopic images were collected using the cellSens Q15 Standard software (Olympus). The ImageJ program was used for the quantification of stain intensity (http://rsb.info.nih.gov/ij/).

The DAB staining solution (1 mg ml^{-1}) and the NBT staining solution (one tablet per 50 ml) were used for analysing the endogenous contents of hydrogen peroxide and superoxide radicals, respectively. Seven-day-old seedlings grown on MS-agar plates at 23 °C were subjected to histochemical staining at 23 or 37 °C for 1 h in complete darkness. The plant samples were then destained with deionized water and visualized by the EOS 5D Mark III camera (Canon). The stain intensity was quantitated using the ImageJ program.

Infrared thermography. Thermal images of 7-day-old seedlings incubated at different temperatures were recorded using the thermal imaging camera T420 (FLIR Systems) and analysed using the FLIR tools (http://www.flirkorea.com/home/).

Transcriptional activation activity assay. A set of reporter and effector plasmids was constructed. The reporter plasmid contains four copies of the GAL4 upstream activation sequence and the β-glucuronidase (GUS) reporter gene. To construct the 35S:*HOS1* effector plasmids, HOS1-coding sequences were fused in-frame to the GAL4 DNA-binding domain-coding sequence, and the fusions were subcloned into an expression vector containing the CaMV 35S promoter. The *HOS1* gene sequences tested include a full-size, an N-terminally truncated and a C-terminally truncated sequences encoding amino acid residues 1–927, 457–927 and 1–457, respectively. *Arabidopsis* mesophyll protoplasts were isolated from 3-week-old Col-0 plants. The reporter and effector plasmids were cotransformed into *Arabidopsis* protoplasts by a polyethylene glycol-calcium transfection method. GUS activities were measured by the fluorometric method, as described previously[40]. A CaMV 35S promoter-luciferase construct was also cotransformed for internal control. The luciferase assay was performed using the luciferase assay system kit (Promega).

HOS1–HSP90 protein interactions. To examine the physical interactions between HOS1 and HSP90, we used yeast two-hybrid screening using the BD Matchmaker system (Takara). The pGADT7 vector was used for GAL4 activation domain and the pGBKT7 vector was used for GAL4 DNA-binding domain. The HOS1-coding sequences were subcloned into the pGBKT7 vector. The HSP90-coding sequence was subcloned into the pGADT7 vector. The yeast strain used for transformation was AH109 (Leu-, Trp-, Ade-, His-), which harbours chromosomally integrated reporter genes encoding β-galactosidase (lacZ) and HIS3 enzyme under the control of the GAL1 promoter. Transformation of yeast cells was performed according to the manufacturer's instruction. Colonies obtained were restreaked on a selective medium lacking Leu, Trp, Ade and His. To prevent non-specific growth of yeast cells, 3-amino-1,2,4-triazole was included in the media at a final concentration of 15 mM.

Bimolecular fluorescence complementation was also used to examine the potential interactions between HOS1 and HSP90. The YFP^N-HOS1 and HSP90-YFP^C constructs were co-expressed transiently in *Arabidopsis* protoplasts by a polyethylene glycol-calcium transfection method. A total of 16 h following cotransfection, the subcellular distribution of HOS1 and HSP90 proteins was visualized by differential interference contrast microscopy and fluorescence microscopy. Reconstitution of YFP fluorescence was observed using the Zeiss LSM510 confocal microscope (Carl Zeiss) with the following YFP filter setup: excitation 513 nm, 458/514 dichroic and emission 560–615 nm bandpass filter.

Trypan blue staining. Dead cells in plant tissues were selectively visualized by trypan blue staining, as described previously[15]. Whole seedlings were soaked in a lactophenol-trypan blue staining solution (10 ml of lactic acid, 10 ml of glycerol, 10 g of phenol, 10 mg of trypan blue, 10 ml of deionized water). The staining solution containing plant samples was boiled for 1 min and incubated overnight at room temperatures. They were then destained by incubating in the destaining solution (lactophenol:ethanol, 1:2) for 30 min at room temperatures.

Statistical analysis. The statistical significance between two means of measurements was determined using the one-sided Student's *t*-test with *P* values of <0.01 or <0.05. To analyse statistical significance for more than two populations, one-way analysis of variance (ANOVA) with post hoc Tukey test ($P < 0.01$) or two-way ANOVA with post hoc Fisher's multiple comparison test ($P < 0.05$) was used. Statistical analyses were performed using the IBM SPSS Statistics 25 software (https://www.ibm.com/).

Reporting Summary. Further information on research design is available in the Nature Research Reporting Summary linked to this article.

Data availability

The raw RNA-seq data generated during this study were deposited in the NCBI Sequence Read Archive (SRA) database under the accession code PRJNA658831. Source data are provided with this paper. The authors declare that any other supporting data are available from the corresponding author upon request.

Received: 4 October 2019; Accepted: 16 October 2020;

References

1. Wanner, L. A. & Junttila, O. Cold-induced freezing tolerance in *Arabidopsis*. *Plant Physiol.* **120**, 391–400 (1999).
2. Wahid, A., Gelani, S., Ashraf, M. & Foolad, M. R. Heat tolerance in plants: an overview. *Environ. Exp. Bot.* **61**, 199–223 (2007).
3. Toivola, D. M., Strnad, P., Habtezion, A. & Omary, M. B. Intermediate filaments take the heat as stress proteins. *Trends Cell Biol.* **20**, 79–91 (2010).
4. Welch, W. J. & Suhan, J. P. Cellular and biochemical events in mammalian cells during and after recovery from physiological stress. *J. Cell Biol.* **103**, 2035–2052 (1986).
5. Boulon, S., Westman, B. J., Hutten, S., Boisvert, F. M. & Lamond, A. I. The nucleolus under stress. *Mol. Cell* **40**, 216–227 (2010).
6. Kantidze, O. L., Velichko, A. K., Luzhin, A. V. & Razin, S. V. Heat stress-induced DNA damage. *Acta Naturae* **8**, 75–78 (2016).
7. Lee, H. et al. The *Arabidopsis* HOS1 gene negatively regulates cold signal transduction and encodes a RING finger protein that displays cold-regulated nucleo-cytoplasmic partitioning. *Genes Dev.* **15**, 912–924 (2001).
8. Lazaro, A. et al. The *Arabidopsis* E3 ubiquitin ligase HOS1 negatively regulates CONSTANS abundance in the photoperiodic control of flowering. *Plant Cell* **24**, 982–999 (2012).
9. Jung, J. H. et al. The cold signaling attenuator HIGH EXPRESSION OF OSMOTICALLY RESPONSIVE GENE1 activates FLOWERING LOCUS C transcription via chromatin remodeling under short-term cold stress in *Arabidopsis*. *Plant Cell* **25**, 4378–4390 (2013).
10. Crawford, A. J., McLachlan, D. H., Hetherington, A. M. & Franklin, K. A. High temperature exposure increases plant cooling capacity. *Curr. Biol.* **22**, R396–R397 (2012).

11. Park, Y. J., Lee, H. J., Ha, J. H., Kim, J. Y. & Park, C. M. COP1 conveys warm temperature information to hypocotyl thermomorphogenesis. *New Phytol.* **215**, 269–280 (2017).
12. Kim, J. H., Lee, H. J., Jung, J. H., Lee, S. & Park, C. M. HOS1 facilitates the phytochrome B-mediated inhibition of PIF4 function during hypocotyl growth in *Arabidopsis*. *Mol. Plant* **13**, 274–284 (2017).
13. Dong, C. H. et al. The negative regulator of plant cold responses, HOS1, is a RING E3 ligase that mediates the ubiquitination and degradation of ICE1. *Proc. Natl Acad. Sci. USA* **103**, 8281–8286 (2006).
14. Mittler, R., Vanderauwera, S., Gollery, M. & Van, B. F. Reactive oxygen gene network of plants. *Trends Plant Sci.* **9**, 490–498 (2004).
15. Menke, M., Chen, I., Angelis, K. J. & Schubert, I. DNA damage and repair in *Arabidopsis thaliana* as measured by the comet assay after treatment with different classes of genotoxins. *Mutat. Res.* **27**, 87–93 (2001).
16. Kobbe, D., Blanck, S., Demand, K., Focke, M. & Puchta, H. AtRECQ2, a RecQ helicase homologue from *Arabidopsis thaliana*, is able to disrupt various recombinogenic DNA structures in vitro. *Plant J.* **55**, 397–405 (2008).
17. Hartung, F., Plchová, H. & Puchta, H. Molecular characterisation of RecQ homologues in *Arabidopsis thaliana*. *Nucleic Acids Res.* **28**, 4275–4282 (2000).
18. MacGregor, D. R. & Penfield, S. Exploring the pleiotropy of hos1. *J. Exp. Bot.* **66**, 1661–1671 (2015).
19. Wang, B. et al. HOS1 regulates Argonaute1 by promoting transcription of the microRNA gene MIR168b in *Arabidopsis*. *Plant J.* **81**, 861–870 (2015).
20. Röhrig, S. et al. The RecQ-like helicase HRQ1 is involved in DNA crosslink repair in *Arabidopsis* in a common pathway with the Fanconi anemia-associated nuclease FAN1 and the postreplicative repair ATPase RAD5A. *New Phytol.* **218**, 1478–1490 (2018).
21. Borges, H. L., Linden, R. & Wang, J. Y. J. DNA damage-induced cell death. *Cell Res.* **18**, 17–26 (2008).
22. Koch, E. & Slusarenko, A. *Arabidopsis* is susceptible to infection by a downy mildew fungus. *Plant Cell* **2**, 437–445 (1990).
23. Swindell, W. R., Huebner, M. & Weber, A. P. Transcriptional profiling of *Arabidopsis* heat shock proteins and transcription factors reveals extensive overlap between heat and non-heat stress response pathways. *BMC Genomics* **8**, 125 (2007).
24. Jantschitsch, C. & Trautinger, F. Heat shock and UV-B-induced DNA damage and mutagenesis in skin. *Photochem. Photobiol. Sci.* **2**, 899–903 (2003).
25. Finka, A. & Goloubinoff, P. Proteomic data from human cell cultures refine mechanisms of chaperone-mediated protein homeostasis. *Cell Stress Chaperones* **18**, 591–605 (2013).
26. Liu, H. C., Liao, H. T. & Charng, Y. Y. The role of class A1 heat shock factors (HSFA1s) in response to heat and other stresses in *Arabidopsis*. *Plant Cell Environ.* **34**, 738–751 (2011).
27. Liu, Z. et al. *Arabidopsis* UVH6, a homolog of human XPD and yeast RAD3 DNA repair genes, functions in DNA repair and is essential for plant growth. *Plant Physiol.* **132**, 1405–1414 (2003).
28. Britt, A. Repair of DNA damage induced by solar UV. *Photosynth. Res.* **81**, 105–112 (2004).
29. Yu, L. et al. Thermopriming triggers splicing memory in *Arabidopsis*. *J. Exp. Bot.* **69**, 2659–2675 (2018).
30. Cheng, Z. et al. Nup96 and HOS1 are mutually stabilized and gate CONSTANS protein level, conferring long-day photoperiodic flowering regulation in *Arabidopsis*. *Plant Cell* **32**, 374–391 (2020).
31. Ellis, R. J., van der Vies, S. M. & Hemmingsen, S. M. The molecular chaperone concept. *Biochem. Soc. Symp.* **55**, 145–153 (1989).
32. Seo, P. J. et al. Cold activation of a plasma membrane-tethered NAC transcription factor induces a pathogen resistance response in *Arabidopsis*. *Plant J.* **61**, 661–671 (2010).
33. Earley, K. W. et al. Gateway-compatible vectors for plant functional genomics and proteomics. *Plant J.* **45**, 616–629 (2006).
34. Ochel, H. J., Eichhorn, K. & Gademann, G. Geldanamycin: the prototype of a class of antitumor drugs targeting the heat shock protein 90 family of molecular chaperones. *Cell Stress Chaperones* **6**, 105–112 (2001).
35. Sharma, S. V., Agatsuma, T. & Nakano, H. Targeting of the protein chaperone, HSP90, by the transformation suppressing agent, radicicol. *Oncogene* **16**, 2639–2645 (1998).
36. Lee, D. H. & Goldberg, A. L. Proteasome inhibitors: valuable new tools for cell biologists. *Trends Cell Biol.* **8**, 397–403 (1998).
37. Lee, S., Seo, P. J., Lee, H. J. & Park, C. M. A NAC transcription factor NTL4 promotes reactive oxygen species production during drought-induced leaf senescence in *Arabidopsis*. *Plant J.* **70**, 831–844 (2012).
38. Gutierrez, L. et al. The lack of a systematic validation of reference genes: a serious pitfall undervalued in reverse transcription–polymerase chain reaction (RT–PCR) analysis in plants. *Plant Biotechnol. J.* **6**, 609–618 (2008).
39. Lee, H. J. et al. FCA mediates thermal adaptation of stem growth by attenuating auxin action in *Arabidopsis*. *Nat. Commun.* **5**, 5473 (2014).
40. Seo, P. J., Kim, M. J., Ryu, J. Y., Jeong, E. Y. & Park, C. M. Two splice variants of the IDD14 transcription factor competitively form nonfunctional heterodimers which may regulate starch metabolism. *Nat. Commun.* **2**, 303 (2011).

Acknowledgements

We thank Y.-Y. Charng for providing the *hsfa1 QK* mutant seeds and D. Somers for providing the *HSP90*-RNAi plants and the ABRC for *Arabidopsis* plant materials. The *RECQ2* cDNA was kindly provided by H. Puchta (Karlsruhe Institute of Technology, Germany). We thank J.-H. Kim for subcloning the *RECQ2* gene and S. Shim for statistical analysis. This work was supported by the Leaping Research (grant no. NRF-2018R1A2A1A19020840) Program provided by the National Research Foundation of Korea (NRF) and the Next-Generation BioGreen 21 Program (PJ013134) provided by the Rural Development Administration of Korea.

Author contributions

C.-M.P. conceived and designed the experiments. C.-M.P. prepared the manuscript with the contributions of S.-H.H. and Y.-J.P. S.-H.H. carried out thermotolerance assays and gene expression and biochemical assays. Y.-J.P. performed data analysis together with S.-H.H. S.-H.H. and Y.-J.P bred and maintained the plant materials. All authors approved the manuscript.

Competing interests

The authors declare no competing interests.

Additional information

Extended data is available for this paper at https://doi.org/10.1038/s41477-020-00809-6.

Supplementary information is available for this paper at https://doi.org/10.1038/s41477-020-00809-6.

Correspondence and requests for materials should be addressed to C.-M.P.

Peer review information *Nature Plants* thanks Chunzhao Zhao and the other, anonymous, reviewer(s) for their contribution to the peer review of this work.

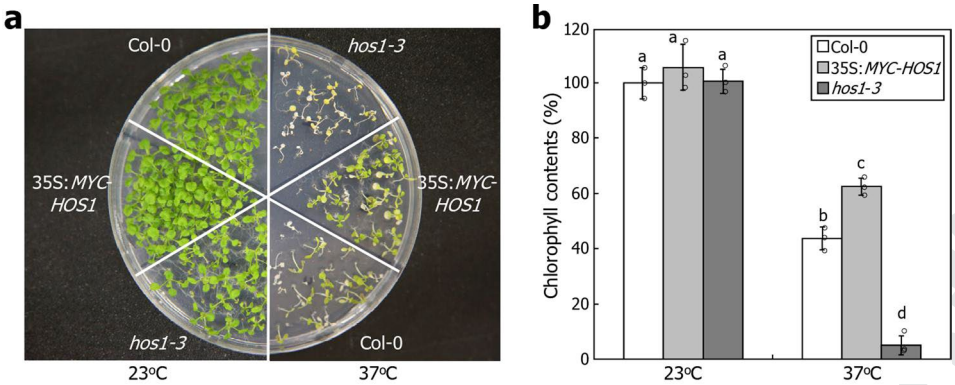

Extended Data Fig. 1 | Thermotolerance phenotypes of 35S:*MYC- HOS1* transgenic plants. Seven-day-old seedlings grown on ½ X Murashige and Skoog-agar (hereafter referred to as MS-agar) plates at 23 °C were exposed to 37 °C for 4 d. Heat-treated seedlings were allowed to recover at 23 °C for 5 d under constant light conditions before taking photograph (**a**). Chlorophyll contents were measured (**b**). Three measurements, each consisting of 15–20 seedlings, were statistically analysed. Error bars indicate standard error of the mean (s.e.m.). Different letters represent significant differences ($P < 0.01$) determined by one-way analysis of variance (ANOVA) with *post hoc* Tukey test. The circles indicate individual datapoints.

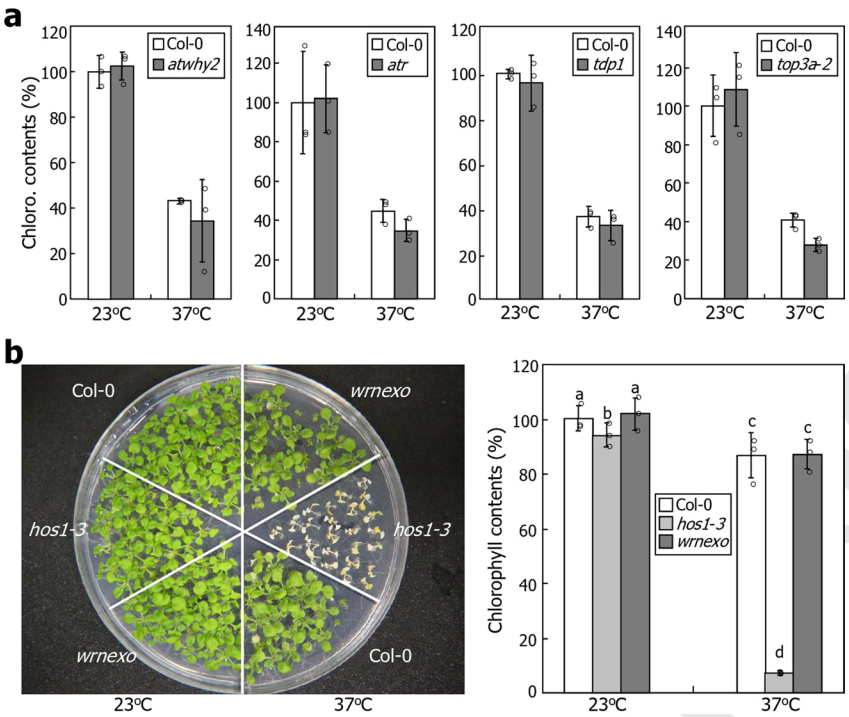

Extended Data Fig. 2 | Relative contents of chlorophylls in DNA damage response- related mutants. Seven-day-old seedlings grown on MS-agar plates at 23 °C were exposed to 37 °C for 1.5 d. The heat-treated seedlings were allowed to recover at 23 °C for 5 d under constant light conditions before measuring chlorophyll contents. Biological triplicates, each consisting of 15–20 seedlings, were statistically analysed. **a**, Chlorophyll contents in DNA damage response-related mutants. The selected mutants are defective in genes that were predicted to be involved in the HOS1- mediated induction of thermotolerance from RNA sequencing analysis (refer to Fig. 2c). The upper side of each boxplot indicates median. Error bars indicate s.e.m. (one-sided *t*-test, $*P < 0.01$, difference from Col-0). The circles indicate individual datapoints. **b**, Thermotolerance phenotypes of *wrnexo* mutant. The RECQ2 protein physically interacts with WERNER SYNDROME-LIKE EXONUCLEASE (WRNexo), a 3'-5' exonuclease that participates in sustaining DNA integrity. Seven-day-old seedlings grown on MS-agar plates at 23 °C were exposed to 37 °C for 1.5 d and then allowed to recover at 23 °C for 10 d under constant light conditions. Biological triplicates, each consisting of 10 seedlings, were statistically analysed. Error bars indicate s.e.m. Different letters represent significant differences ($P < 0.01$) determined by one-way ANOVA with *post hoc* Tukey test. The circles indicate individual datapoints.

a

P1
(-1809) 5′-ATATATATATTTTTTTCCAAAAGTTAACGGTAAATAACTCAATATATATAGATATATAACTCGATCACCTTACTTA
TTTATCTAATAAATTTATAAACATTACTCAATATCCTGAAAAATTGAGTTAAACTAGTCATG (-1669)

P2
(-1542) 5′-TTTATAAAACTTACTCGGTTTTTTTGATAACCTAACTCCTTTGGTTAGTAGTTAATTTCCTTCGTTTTGCTTTTCCA
ATTCTATGCATATTGTTTTAACCATTTTATTACTCCGTTTCCGTTTGTTTCACTACAATTATTTGGAGCTACAGT (-1389)

P3
(-1347) 5′-TCTTGGGAAACACTTGCCCTTTGACTGGATTTGTTATATTAAAAATTGTGCAAGCACGTGTTTGCTAAAATTTAAAAT
GAGAAGCTGTGAGCTAAAAGCTTCGCTGTTAGGTTCATCAACTAGTCTGTCTGGTGCTTCAAAGGAAT (-1203)

P4
(-847) 5′-ACTTTTCAAATAGGTCATTTGGAGATATATCACATATCGAACGAATCCATGATCCCTCCAGGCTTCATCCAGTTCACT
TTGACCTCACTCACTCTTCTTCTTTCTTTCAGAAAATGATTTATATAACTTTTCTTCTTCTTTTAAACATATATAT (-690)

P5
(-684) 5′-TTTTTTATAATAATTTCTATAGAATTCTTTTAATATATATATCCACAAATCCACATAGTTTTGAATAATCTTTAGATA
AACTAGTCCTCTCCTTCGATGAATACTTCACGCGTACTAGTTTTTTTTCTTCATGAATACTTGTCGTTGTGATGCAGCA (-527)

b

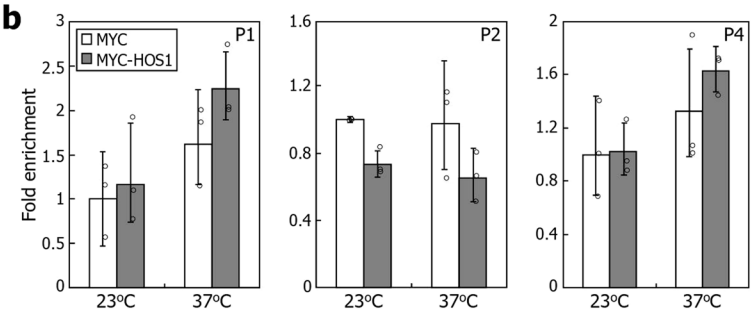

Extended Data Fig. 3 | HOS1 binding to *RECQ2* promoter. a, *RECQ2* promoter sequences examined in chromatin immunoprecipitation (ChIP)-qPCR. The conserved G-box and GATA-box sequences were underlined in green and blue, respectively. **b**, Control data for ChIP-qPCR assays. The assays were performed under the assay conditions identical to those described in Fig. 3f. The measurements were statistically analysed, as described in Fig. 3f. Error bars indicate standard deviation from the mean (SD). The data with P1, P2, and P4 sequence elements were displayed. The circles indicate individual datapoints.

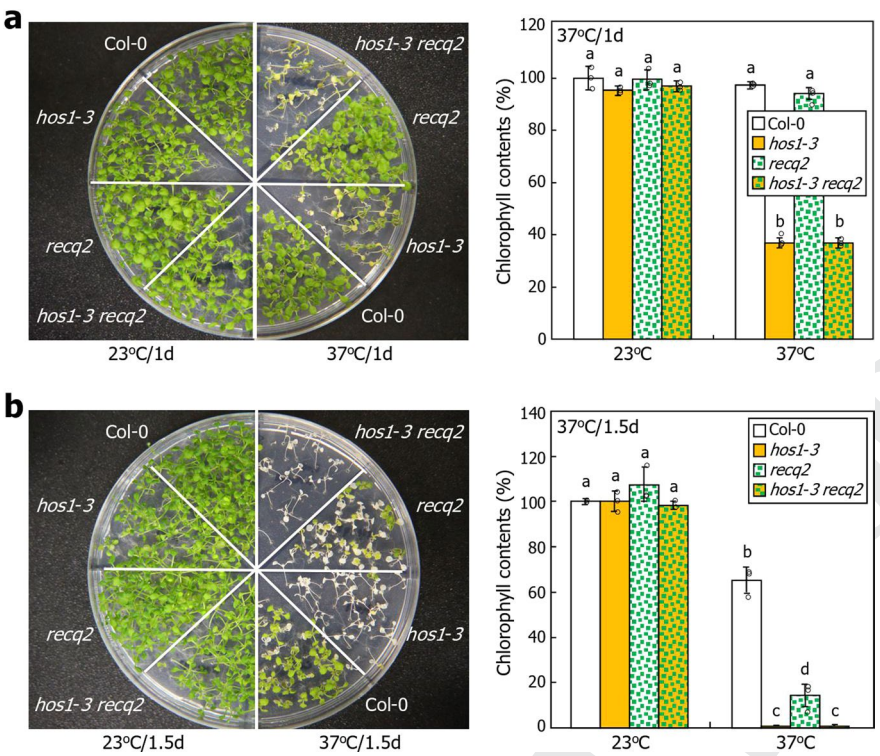

Extended Data Fig. 4 | Thermotolerance phenotypes of *hos1-3 recq2* double mutant. Seven-day-old seedlings grown on MS-agar plates at 23 °C were exposed to 37 °C for either 1 d (**a**) or 1.5 d (**b**) and then allowed to recover at 23 °C for 5 d under constant light conditions (left photographs). Chlorophyll contents were measured (right graphs). Biological triplicates, each consisting of 10 seedlings, were statistically analysed. Error bars indicate s.e.m. Different letters represent significant differences ($P < 0.01$) determined by one-way ANOVA with *post hoc* Tukey test. The circles indicate individual datapoints.

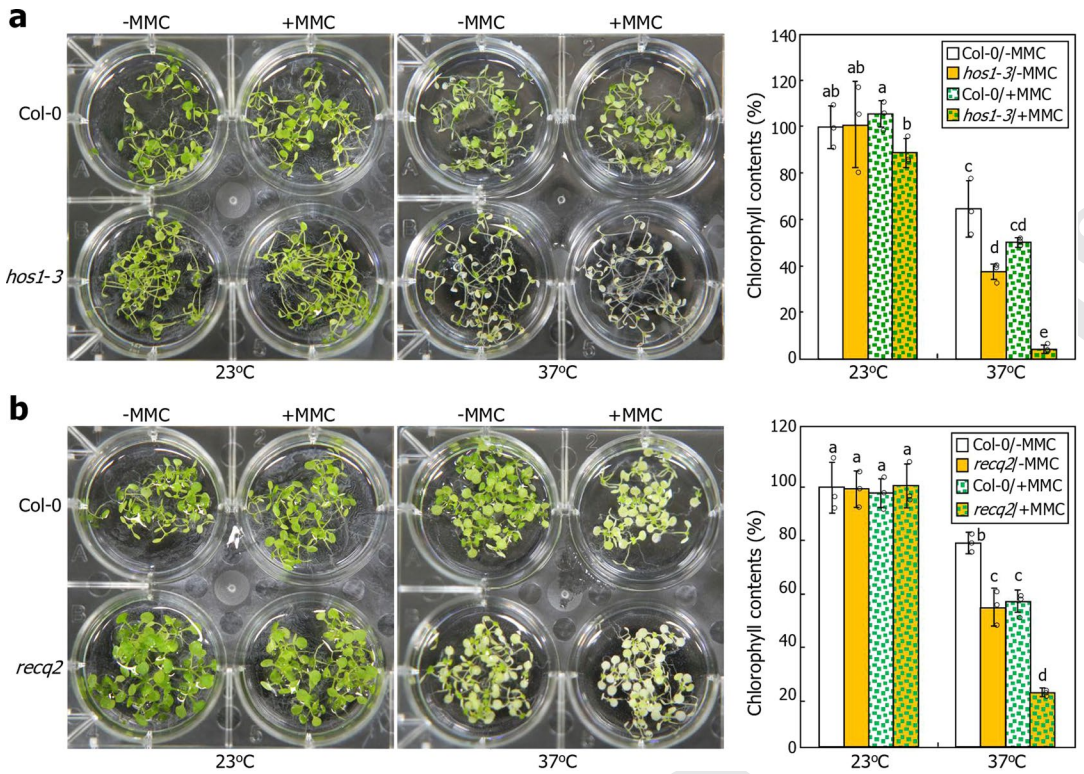

Extended Data Fig. 5 | Effects of mitomycin on thermotolerance. a, Thermotolerance phenotypes of *hos1-3* mutant in the presence of mitomycin (MMC). Seven-day-old seedlings grown on MS-agar plates at 23 °C were transferred to liquid MS cultures containing 10 μg/ml MMC, which is known to damage DNA molecules by inducing cross-linking of nucleotides, and exposed to 37 °C for 1 d. Heat-treated seedlings were allowed to recover at 23 °C for 5 d under constant light conditions (left photographs). Three measurements of chlorophyll contents, each consisting of 15–20 seedlings, were statistically analysed (right graph). Error bars indicate s.e.m. Different letters represent significant differences ($P < 0.05$) determined by two-way ANOVA with *post hoc* Fisher's multiple comparison test. **b**, Thermotolerance phenotypes of *recq2* mutant in the presence of MMC. Heat-treated seedlings were allowed to recover at 23 °C for 10 d under constant light conditions (left photographs). Chlorophyll contents were measured and statistically analysed (right graph), as described above. The circles indicate individual datapoints.

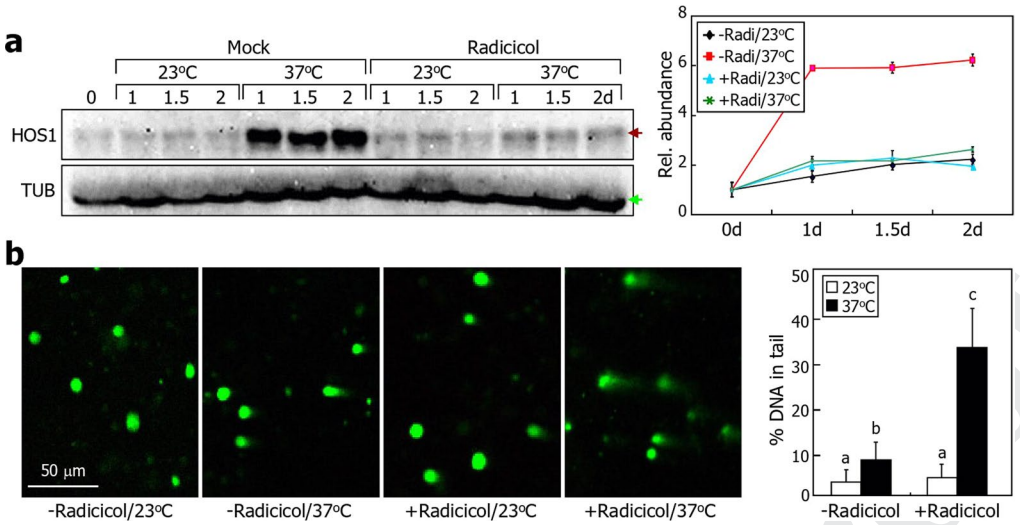

Extended Data Fig. 6 | Effects of radicicol on the thermal accumulation of HOS1 proteins and genomic integrity. a, Effects of radicicol on the thermal accumulation of HOS1 proteins. Seven-day-old 35S:*MYC-HOS1* transgenic seedlings grown on MS-agar plates at 23 °C were transferred to 37 °C and subjected to treatments with 10 μM radicicol, an antibiotic inhibitor of HSP90. The MYC-HOS1 proteins were immunologically detected using an anti-MYC antibody. TUB proteins were assayed in parallel for loading control. Brown arrows mark 112 kDa, and green arrows mark 50 kDa. d, day. Immunoblots were quantitated using the ImageJ software, and three quantitations were statistically analysed. The dotplots indicate median. Error bars indicate SD. **b**, Comet assays in the presence of radicicol. Seedling growth, heat treatments, and comet assays were performed, as described in Fig. 2e. DNA breaks were quantitated by measuring the tail ratio of total fluorescence intensity in comet-shaped DNA spots. DNA spots of 8–12 were statistically analysed. Error bars indicate SD. Different letters represent significant differences ($P < 0.01$) determined by one-way ANOVA with *post hoc* Tukey test.

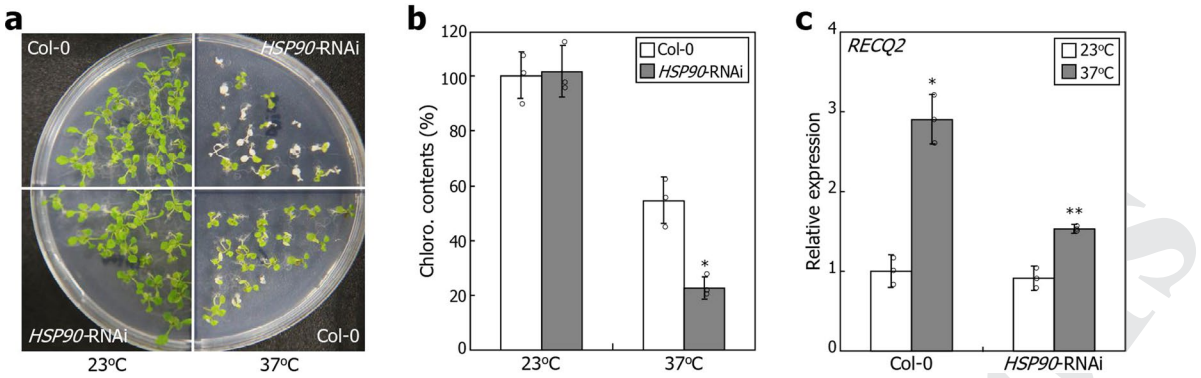

Extended Data Fig. 7 | Thermotolerance phenotypes of *HSP90*- RNAi plants. a, **b**, Thermotolerance phenotypes. Seven-day-old seedlings grown on MS-agar plates at 23 °C were exposed to 37 °C for 2 d. Heat-treated seedlings were allowed to recover at 23 °C for 5 d under constant light conditions before taking photograph (**a**). Chlorophyll contents were measured (**b**). Three measurements, each consisting of 15–20 seedlings, were statistically analysed using one-sided Student's *t*-test (*$P = 0.008$, difference from Col-0). **c**, Transcription of *RECQ2* gene. Seven-day-old seedlings grown on MS-agar plates at 23 °C were exposed to 37 °C for 2 d. Whole seedlings were used for total RNA preparation. Transcript levels were analysed by RT- qPCR. Biological triplicates, each consisting of 15 seedlings, were statistically analysed (one-sided *t*-test, *$P = 0.0005$, **$P = 0.0007$, difference from 23 °C). In **b** and **c**, the upper side of each boxplot indicates median. Error bars indicate s.e.m. The circles indicate individual datapoints.

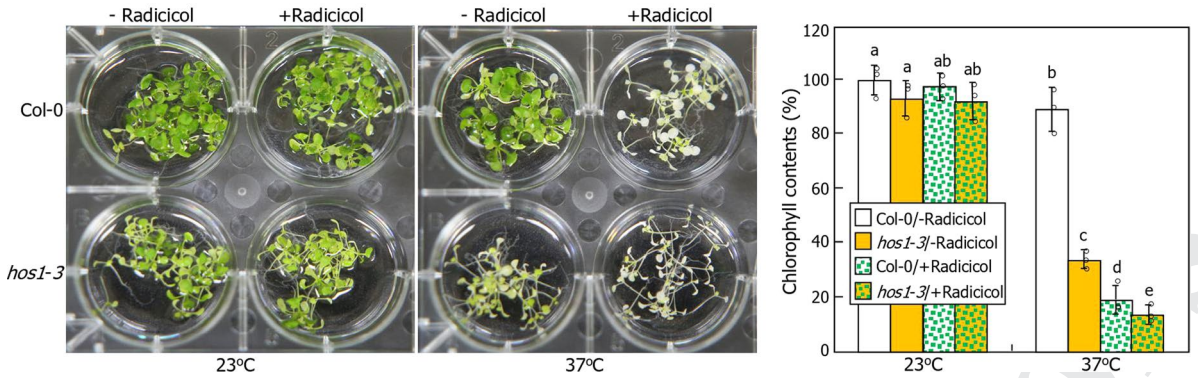

Extended Data Fig. 8 | Thermotolerance phenotypes of *hos1-3* mutant in the presence of radicicol. Seven-day-old seedlings grown on MS-agar plates at 23 °C were transferred to liquid MS cultures containing 10 μM radicicol and exposed to 37 °C for 1 d. Heat-treated seedlings were allowed to recover at 23 °C for 5 d under constant light conditions. Three measurements of chlorophyll contents, each consisting of 15–20 seedlings, were statistically analysed. Error bars indicate s.e.m. Different letters represent significant differences ($P < 0.05$) determined by two-way ANOVA with *post hoc* Fisher's multiple comparison test. The circles indicate individual datapoints.

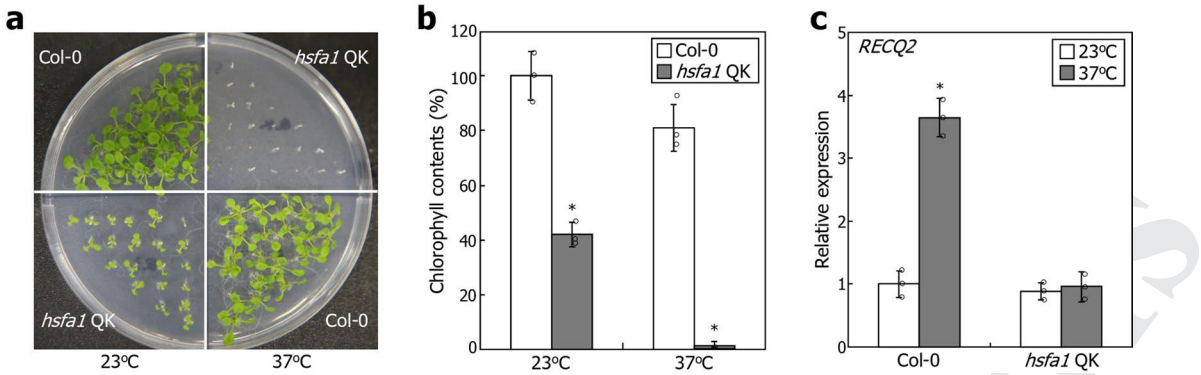

Extended Data Fig. 9 | Thermotolerance phenotypes of *hsfa1a/hsfa1b/hsfa1d/ hsfa1e* quadruple knockout (*hsfa1* QK) mutant. a, **b**, Thermotolerance phenotypes. Seven-day-old *hsfa1* QK mutant seedlings grown on MS-agar plates at 23 °C were exposed to 37 °C for 1 d. Heat-treated seedlings were allowed to recover at 23 °C for 5 d under constant light conditions before taking photograph (**a**). Chlorophyll contents were measured (**b**). Three measurements, each consisting of 15–20 seedlings, were statistically analysed using one-sided Student's *t*-test (*$P = 0.004$, difference from Col-0). **c**, Transcription of *RECQ2* gene. Seven-day-old seedlings grown on MS-agar plates at 23 °C were exposed to 37 °C for 1 d. Whole seedlings were used for total RNA preparation. Transcript levels were analysed by qRT–PCR. Biological triplicates, each consisting of 15 seedlings, were statistically analysed (one-sided *t*-test, *$P = 0.0002$, difference from 23 °C). In **b** and **c**, the upper side of each boxplot indicates median. Error bars indicate s.e.m. The circles indicate individual datapoints.

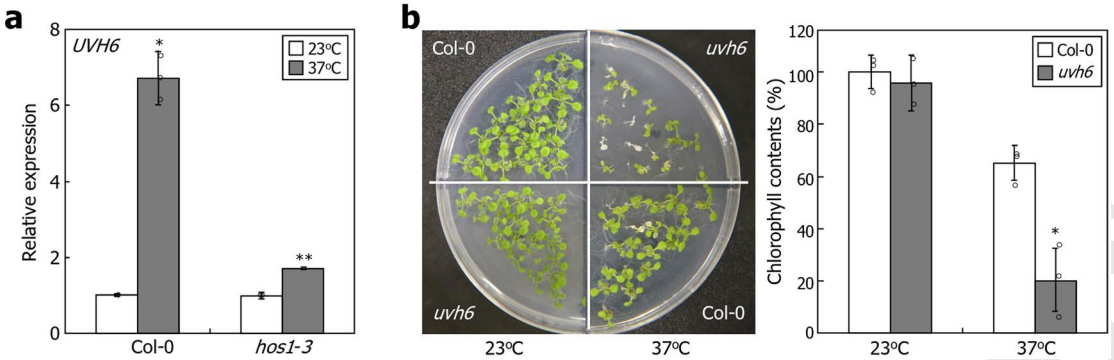

Extended Data Fig. 10 | Thermotolerance phenotypes of *uvh6* mutant. a, Transcription of *ULTRAVIOLET HYPERSENSITIVE 6* (*UVH6*) gene in *hos1-3* mutant at high temperatures. Seven-day-old seedlings grown on MS-agar plates at 23 °C were exposed to 37 °C for 1.5 d. Total RNA samples were extracted from whole seedlings. Transcript levels were analysed by qRT–PCR. Biological triplicates, each consisting of 15 seedlings, were statistically analysed using one-sided Student's *t*-test (**P* = 0.0019, ***P* = 0.0017, difference from 23 °C). The upper side of each boxplot indicates median. Error bars indicate s.e.m. The circles indicate individual datapoints. **b**, Thermotolerance phenotypes of *uvh6* mutant. Seven-day-old UVH6-deficient *uvh6* mutant grown on MS-agar plates at 23 °C were exposed to 37 °C for 1.5 d and then allowed to recover at 23 °C for 5 d under constant light conditions (left photographs). Chlorophyll contents were measured (right graph). Biological triplicates, each consisting of 10 seedlings, were statistically analysed (one-sided *t*-test, **P* = 0.002, difference from Col-0). The upper side of each boxplot indicates median. Error bars indicate s.e.m. The circles indicate individual datapoints.

QUERY FORM

Nature Plants	
Manuscript ID	**[Art. Id: 809]**
Author	**Shin-Hee Han**

AUTHOR:

The following queries have arisen during the editing of your manuscript. Please answer by making the requisite corrections directly in the e.proofing tool rather than marking them up on the PDF. This will ensure that your corrections are incorporated accurately and that your paper is published as quickly as possible.

Query No.	*Nature of Query*
Q1:	Please note, we reserve 'significant' and its derivatives for statistical significance. Please reword where this is not the intended meaning (for example to important, notable, substantial); there are 6 possible instances throughout your text.
Q2:	Fig. 1d: please define FW in caption - fresh weight?
Q3:	Please check your article carefully, coordinate with any co-authors and enter all final edits clearly in the eproof, remembering to save frequently. Once corrections are submitted, we cannot routinely make further changes to the article.
Q4:	Note that the eproof should be amended in only one browser window at any one time; otherwise changes will be overwritten.
Q5:	Author surnames have been highlighted. Please check these carefully and adjust if the first name or surname is marked up incorrectly. Note that changes here will affect indexing of your article in public repositories such as PubMed. Also, carefully check the spelling and numbering of all author names and affiliations, and the corresponding email address(es).
Q6:	You cannot alter accepted Supplementary Information files except for critical changes to scientific content. If you do resupply any files, please also provide a brief (but complete) list of changes. If these are not considered scientific changes, any altered Supplementary files will not be used, only the originally accepted version will be published.
Q7:	If applicable, please ensure that any accession codes and datasets whose DOIs or other identifiers are mentioned in the paper are scheduled for public release as soon as possible, we recommend within a few days of submitting your proof, and update the database record with publication details from this article once available.
Q8:	Fig. 2b - Please explain meaning of 2E-3 to 2E-8 shading used in figure.
Q9:	The program name 'caslab' has been replaced with 'casplab' throughout - please confirm that this is correct.
Q10:	We have altered the x axes of many parts of Fig. 3 by adding an axis label of 'Temperature (°C)' per journal style. Please check and confirm this is correct.
Q11:	In Fig. 4 caption the repeat description for g has been deleted. Please check that the text is now correct.
Q12:	In the sentence beginning, 'In addition, the hsfa1 QK mutant seedlings...' 'RNAi' has been spelt out as 'RNA interference' at first use, according to journal style.

QUERY FORM

Nature Plants	
Manuscript ID	**[Art. Id: 809]**
Author	**Shin-Hee Han**

AUTHOR:

The following queries have arisen during the editing of your manuscript. Please answer by making the requisite corrections directly in the e.proofing tool rather than marking them up on the PDF. This will ensure that your corrections are incorporated accurately and that your paper is published as quickly as possible.

Query No.	*Nature of Query*
Q13:	In the sentence beginning, 'The transfer DNA insertional knockout mutants,...' 'T-DNA' has been spelt out at first use, in keeping with journal style.
Q14:	In the sentence beginning, 'Analysis of transcript levels ...' the phrase 'reverse transcription-mediated quantitative PCR (RT-qPCR)' has been replaced with 'quantitative PCR with reverse transcription (qRT-PCR)' in keeping with journal style. Throughout the text, RT-qPCR has accordingly been changed to qRT-PCR.
Q15:	In the sentence beginning, 'The ImageJ program...' the link appears to have been updated to https://imagej.nih.gov/ij/ - should this be substituted?
Q16:	Reference [39] is a duplicate of [15] and hence the repeated version has been deleted. Please check.

nature research

Corresponding author(s): Chung-Mo Park

Last updated by author(s): Oct 12, 2020

Reporting Summary

Nature Research wishes to improve the reproducibility of the work that we publish. This form provides structure for consistency and transparency in reporting. For further information on Nature Research policies, see our Editorial Policies and the Editorial Policy Checklist.

Statistics

For all statistical analyses, confirm that the following items are present in the figure legend, table legend, main text, or Methods section.

n/a	Confirmed	
☐	☒	The exact sample size (*n*) for each experimental group/condition, given as a discrete number and unit of measurement
☐	☒	A statement on whether measurements were taken from distinct samples or whether the same sample was measured repeatedly
☐	☒	The statistical test(s) used AND whether they are one- or two-sided *Only common tests should be described solely by name; describe more complex techniques in the Methods section.*
☒	☐	A description of all covariates tested
☒	☐	A description of any assumptions or corrections, such as tests of normality and adjustment for multiple comparisons
☐	☒	A full description of the statistical parameters including central tendency (e.g. means) or other basic estimates (e.g. regression coefficient) AND variation (e.g. standard deviation) or associated estimates of uncertainty (e.g. confidence intervals)
☐	☒	For null hypothesis testing, the test statistic (e.g. *F*, *t*, *r*) with confidence intervals, effect sizes, degrees of freedom and *P* value noted *Give P values as exact values whenever suitable.*
☒	☐	For Bayesian analysis, information on the choice of priors and Markov chain Monte Carlo settings
☒	☐	For hierarchical and complex designs, identification of the appropriate level for tests and full reporting of outcomes
☒	☐	Estimates of effect sizes (e.g. Cohen's *d*, Pearson's *r*), indicating how they were calculated

Our web collection on statistics for biologists contains articles on many of the points above.

Software and code

Policy information about availability of computer code

Data collection	QuantStudio Real-Time PCR software V1.1 (Life Technologies), MikroWin 2010 (Berthold Technologies), Nanodrop 2000 (Thermo Fisher Scientific, cat. ND-2000c), Fusion Molecular Imaging V15.18 (Vilber Lourmat), Olympus cellSens Standard V1.16 (Olympus), Zen 2 blue edition (Carl ZEISS), Casplab comet 1.2.3b2 (http://caslab.com/), NCBI primer-BLAST software (https://www.ncbi.nlm.nih.gov/tools/primer-blast/index.cgi)
Data analysis	QuantStudio Real-Time PCR software V1.1 (Life Technologies), ImageJ V1.52, Microsoft Excel 2003, Casplab comet 1.2.3b2 (http://caslab.com/), FLIR Tools software (FLIR), BINGO V3.0.0, IBM SPSS Statistics 25

For manuscripts utilizing custom algorithms or software that are central to the research but not yet described in published literature, software must be made available to editors and reviewers. We strongly encourage code deposition in a community repository (e.g. GitHub). See the Nature Research guidelines for submitting code & software for further information.

Data

Policy information about availability of data

All manuscripts must include a data availability statement. This statement should provide the following information, where applicable:

- Accession codes, unique identifiers, or web links for publicly available datasets
- A list of figures that have associated raw data
- A description of any restrictions on data availability

All data and transgenic lines are available through contacting corresponding authors. The RNA-Seq data reported here has been deposited in the NCBI's SRA database with accession number of PRJNA658831.

Field-specific reporting

Please select the one below that is the best fit for your research. If you are not sure, read the appropriate sections before making your selection.

☒ Life sciences ☐ Behavioural & social sciences ☐ Ecological, evolutionary & environmental sciences

For a reference copy of the document with all sections, see nature.com/documents/nr-reporting-summary-flat.pdf

Life sciences study design

All studies must disclose on these points even when the disclosure is negative.

Sample size	Sample size was determined in a way that we are able to obtain statistically significant differences from at least 3 biological replicates. For thermotolerance phenotype analysis by measuring chlorophyll contents, 10-25 seedlings were analyzed for each genotype. For survival rate analysis, 40-50 seedlings were analyzed for each assay. For other biochemical analyses, 10-20 seedlings were used for each assay.
Data exclusions	We excluded seedlings that exhibited overall growth defects prior to heat treatments. We reasoned that these abnormal seedlings caused either by delayed seed germination or defective developmental conditions are not directly related to the genotypes examined. In comet assays, we excluded abnormal nuclei that did not exhibit intact comet shapes nor round shapes. It was pre-established that the software itself excludes incomplete comet shapes, which is widely accepted in the community.
Replication	For measurements of chlorophyll contents, qRT-PCR, RNA-seq, transcriptional activation activity assay, western protein assay, and comet assay, three independent measurements were statistically analyzed. For thermal accumulation of ROS and trypan blue staining, 8 and 10 representative rosette leaves were statically analyzed, respectively. Similar patterns and data were obtained from repeated assays.
Randomization	For each experiment, we put randomly MS-agar plates, on which multiple seed genotypes were germinated, in a growth chamber or culture room in a way that each seed pool is randomly exposed to heat treatments.
Blinding	Each experiment was blinded and performed by different coauthors and other researchers.

Reporting for specific materials, systems and methods

We require information from authors about some types of materials, experimental systems and methods used in many studies. Here, indicate whether each material, system or method listed is relevant to your study. If you are not sure if a list item applies to your research, read the appropriate section before selecting a response.

Materials & experimental systems

n/a	Involved in the study
☐	☒ Antibodies
☒	☐ Eukaryotic cell lines
☒	☐ Palaeontology and archaeology
☒	☐ Animals and other organisms
☒	☐ Human research participants
☒	☐ Clinical data
☒	☐ Dual use research of concern

Methods

n/a	Involved in the study
☒	☐ ChIP-seq
☒	☐ Flow cytometry
☒	☐ MRI-based neuroimaging

Antibodies

Antibodies used	Anti-MYC (Millipore, mouse monoclonal, cat. 05-724, 1:2000), anti-H3Ac (Millipore, rabbit polyclonal, cat. 06-599, 1:2000), anti-HSP90.1 (Millipore, mouse monoclonal, cat. 05-594, 1:2000), anti-HOS1 (AbClon, rabbit polyclonal, 1:2000, ref; Jung et al. The Plant Cell, 25: 4378–4390, 2013), anti-alpha- tubulin (Sigma-Aldrich, mouse monoclonal, cat. T9026, 1:2000), goat anti-mouse IgG-HRP (Millipore, cat. AP124P, 1:5000), and goat anti-rabbit IgG-HRP (Millipore, cat. AP132P, 1:5000) antibodies.
Validation	The antibodies used, except for anti-HOS1 antibody, are commercially available and experimentally validated by the supplier: Delivering high-quality antibodies requires us to perform rigorous specificity and sensitivity testing in order to provide our customers with reliable tools that generate consistent results. Our standard antibody validation processes include verification for each recommended immunodetection application. All of the thousands of antibodies in or portfolio are certified through our standard validation process to ensure quality and reproducibility.